

Analyzing mixing quality in a curved centrifugal micromixer through numerical simulation



Amir Shamloo*, Parham Vatankhah, Ali Akbari

Department of Mechanical Engineering, Sharif University of Technology, Azadi Ave., Tehran, Iran

ARTICLE INFO

Article history:

Received 12 September 2016

Received in revised form 16 February 2017

Accepted 16 March 2017

Available online 18 March 2017

Keywords:

Micromixer

Microchannel

Secondary flow

Mixing quality

ABSTRACT

The Lab On a CD (LOCD), also known as Centrifugal Microfluidics, has evolved into a sophisticated platform for performing biomedical assays due to its marvelous miniaturization and accurate simulation of biological reactions. Among the numerous applications of the LOCD is fluid mixing. In this paper a centrifugal, serpentine micromixer is simulated and reformed toward better mixing performance. The micromixer was chosen to be curved as a curved design was found to be thrice as functional and compact as a rectilinear design, mixing-wise. The two angular velocity and opening radius parameters were originally hypothesized to affect mixing performance. Effect of angular velocity was studied over a broad range starting from quite low values. It was gathered that with increasing angular velocity, mixing performance initially drops and upon reaching a minimum at a threshold angular velocity, begins to continuously increase. The threshold angular velocity was found to be the spot at which the mixing regime changes from diffusion to secondary flow. It was also realized that increasing the opening radius enhances mixing performance only insignificantly, such that it would not be a practical means of making micromixers more efficient.

© 2017 Elsevier B.V. All rights reserved.

1. Introduction

The Lab-On-A-Chip (LOC) is a microfluidic miniaturization platform used in many chemical, biological and biomedical assays; e.g. the Point Of Care Testing (POCT) (Figeys and Pinto [1], Haeberle et al. [2], Lee and Choi [3], Chin et al. [4], Ryu et al. [5]). Because of its small dimensions, the amount of the consumed sample and reagent is significantly less than other known experimental platforms; i.e. nanoliters vs. milliliters, making the LOC extremely efficient concerning material expenses (Srinivasan et al. [6], Fair [7]). Several modules or operational units could be erected on the LOC for various applications in biological assays such as mixing, valving and separation (Strohmeier et al. [8]). The problem with the LOC is that each operational unit requires a separate micropump, mostly syringe pumps, as its driving force to operate. For this reason, multifunctional LOCs are rather scarce since employing several micropumps in an LOC complexes its design, making it harder to fabricate. To overcome the limitation on multifunctionality, the Lab-On-A-CD (LOCD) was introduced. The LOCD is also a microfluidic miniaturization platform which is a

rotating disk in the shape of a CD [9]. Through use of the centrifugal force induced due to the rotation of the platform around its central axis, the LOCD does not require a micropump for the propelling movement of the fluid. All operational units within an LOCD such as mixing, separation, valving, droplet generating, and etc. could operate using a single rotational motor [10–13]. The disk is mounted on a shaft through the CD hole and the shaft's rotation generates centrifugal force within the fluid, propelling it from the input through the operational units and toward the output [14].

Due to the simplicity of its design, the LOCD is a convenient platform when it comes to biomedical assays such as biochemical and enzymatic studies (Lee et al. [15], Kim et al. [16], Lai et al. [17]), DNA studies (Jia et al. [18]) and POCT (Gorkin et al. [19]). For such analyses to occur, operational units such as valving (Madou et al. [20]) and mixing (Noroozi et al. [21]) units are developed for the LOCD (Chakraborty [22]).

If any chemical reaction is to be effective, first the reagents of that reaction need be thoroughly mixed. In large scales, fluid mixing is achieved rather simply through available solutions. However, it still remains a challenge to achieve a proper mixing of two fluids in microfluidic scales. In microfluidic systems the fluid flow is greatly laminar and the Reynolds number is rather small, hence, there can be no turbulent mixing occurring due to the natural stirring of the fluid caused by turbulence vortices.

* Corresponding author.

E-mail address: shamloo@sharif.edu (A. Shamloo).

There are two general types of micromixers: active and passive. Active micromixers utilize an external energy source or force field such as magnetic (Wang et al. [23]) or electrical (Wu and Liu [24]) to operate. Passive micromixers, however, simply rely on the geometry of the LOCD design (Tofteberg et al. [25], Hessel et al. [26]).

A pressure-driven, passive micromixer for mixing fluids at rather small Reynolds numbers was developed by Stroock et al. [27]. Special obstacles were embodied in the microchannel floor such that the fluids would be mixed upon flowing over them. Multiple micromixers were devised for the LOCD [28–33]. Current micromixers mostly do not show appropriate mixing performance in spite of their rather complex design. A centrifugal micromixer was introduced by Haerberle et al. [2] which was implemented on a straight, radial microchannel. This micromixer functioned based on the transverse flow created due to the Coriolis force which is one of the main volume forces exerted on the fluid within an LOCD. Despite having a quite simple design, their micromixer had limited mixing performance since it was extremely dependent on the LOCD's angular velocity and its resulting Coriolis force. Batch-mode mixing in an LOCD was achieved by Grumman et al. [10] through distributing magnetic particles within the two to-be-mixed fluids. A reciprocating micromixer consisting of two reservoirs connected via U-shaped microchannels was devised by Noroozi et al. [21] which had a high mixing performance. However, due to its geometric limitations, implementing this micromixer in an integrated LOCD setting faces complications. Serpentine microchannel arrangements within an LOCD were introduced by Duffy et al. [34], Puckett et al. [35] and Zoval and Madou [36] for enzymatic, bacterial and protein-ligand analyses, respectively. Their serpentine design was employed only to lengthen the flow path such that the fluid had enough time to freely diffuse. By securing the necessary diffusion time, sufficient mixing was ensured. Yet a thorough observation of the mixing process was not given.

For an LOCD to be used in POCT diagnostics it should most of all be disposable; Therefore, its fabrication should be simple and cost-effective. Hence, as long as a sufficient mixing performance is ensured, a simple passive design without any additional components such as electrodes or magnets is preferred to rather complex active designs. Such simple passive design is conveniently fabricated (even in mass-production scales), portable, cost-effective and easy to use. A centrifugal serpentine micromixer (CSM) was developed by La et al. [37] for an LOCD platform. They compared the CSM and its mixing performance with a pressure-driven serpentine micromixer (PSM). The PSM yielded limited mixing performance since the two laminar flows within it could only mix through diffusion and inertial stirring effects occurring within the microchannel's sharp corners. Yet the CSM showed superior mixing performance due to having an additional secondary flow caused by the Coriolis force. To find a direct approach for quantifying mixing performance is greatly appreciated. However, this goal is not simply achieved for there are many micromixers available and yet no standard criterion exists for determining mixing performance in them all. (Falk and Commenge [38]). Because of this, several studies were conducted in the past couple of years in order to define a quantified index resembling mixing performance. Experimental methods were employed in a couple of these aforementioned studies such as particular chemical reactions and fluorescent microscopy (Ehrfeld et al. [39], Falk and Commenge [38]). Although they grant qualitative analyses of mixing in micromixers, they are unable to offer a quantitative assay such as mixing length or mixing time data (Aubin et al. [40]).

Methods previously used to evaluate the mixing performance of macromixers were employed for the same purpose in

micromixers. One of them applied a Lagrangian analysis in following two to-be-mixed fluid streams (Zalc et al. [41]). The concentration distribution was statistically analyzed at each section of the mixer, thus quantifying the mixture's homogeneity. This analysis was derived from Danckwerts' "intensity of segregation" concept which calculates the variance of the concentration (σ^2_c) with respect to its mean (c_{avg}) throughout different locations (Danckwerts [42]). Shamloo et al. adopted the mixing quality term from this concept and implemented it in their study to quantify mixing performance (Shamloo et al. [43]). They investigated the mixing quality of a centrifugal, serpentine micromixer employed on an LOCD through multiple different setups. The effect of several design parameters of the LOCD including inlet angle, angular velocity and cross-sectional profile was studied on the mixing quality. Their designed microchannel was rectilinear and had sharp corners in microchannel turns.

In this paper, a curved microchannel is devised instead and the effect of the new curved geometry on the mixing quality is investigated. Secondly, the mixing behavior is studied over a broad range of angular velocities to acquire a profound understanding of the effect of this critical parameter on mixing quality in LOCDs. Finally, the effect of the opening radius at which the microchannel starts (from the origin of coordinates being the LOCD's center) on the mixing quality is assessed.

2. Numerical formulation and governing equations

Three well-known PDEs govern the physics of the presented micromixer problem. The incompressible, steady-state Navier-Stoke's momentum equations and the incompressible, steady-state continuity equation govern the fluid flow while the fluid is considered to be Newtonian with constant properties. Also the steady-state, constant-diffusivity convection-diffusion equation directs the concentration distribution within the medium. Having applied the aforementioned assumptions, the governing equations are given as Eq. (1) through Eq. (3):

$$\rho(\nabla \cdot \mathbf{u}) = -\nabla P + \mu \nabla^2 \mathbf{u} + \mathbf{f}^b \quad (1)$$

$$\nabla \cdot \mathbf{u} = 0 \quad (2)$$

$$\mathbf{u} \cdot \nabla c = D \nabla^2 c \quad (3)$$

all above equations are numerically solved in three dimensions. In these equations, \mathbf{u} is the velocity vector (m/s), c is the concentration (mol/m³) and they both are the unknown variables for which the equations are solved. P and \mathbf{f}^b denote pressure (Pa) and volumetric force vector (N/m³), respectively. Finally, the constants ρ , μ and D are material constants indicating fluid density (kg/m³), dynamic viscosity (Pa s) and diffusivity constant (m²/s). The volumetric force vector here is the vector sum of the centrifugal and Coriolis volumetric forces generated due to the angular motion of the LOCD and is given in Eq. (4).

$$\mathbf{f}^b = -\rho \vec{\omega} \times (\vec{\omega} \times \mathbf{r}) - 2\rho \vec{\omega} \times \mathbf{u} \quad (4)$$

where $\vec{\omega}$ denotes the LOCD's angular velocity vector. As was mentioned earlier, the index appropriate for indication of mixing performance is the Mixing Quality (M.Q.) which is calculated as follows in Eq. (5) through Eq. (6):

$$\text{CoV} = \frac{\sqrt{\sum_{i=1}^n (c_i - c_{avg})^2}}{c_{avg}} \quad (5)$$

$$M.Q. = 1 - CoV \quad (6)$$

here, CoV is the Coefficient of Variation which is calculated for the concentration profile. n is the number of data points acquired via discretization of the cross sections on which concentration was read. c_{avg} is the mass-flow weighted average of the concentration calculated over the concentration profile at desired microchannel cross-section. The resulting M.Q. is a number between 0 and 1, where 0 indicates no mixing at all and 1 indicates ideal mixing.

Aside from the Mixing Quality, the dimensionless Reynolds number (Re) could also describe a micromixer's operation (Malecha et al. [44]). This dimensionless numbers is defined as Eq. (7):

$$Re = \frac{\rho u_{avg} D_h}{\mu} \quad (7)$$

where u_{avg} is the mean velocity (m/s) and D_h is the microchannel's hydraulic diameter (m) which itself is obtained as follows in Eq. (8):

$$D_h = \frac{4A_c}{P_w} \quad (8)$$

in Eq. (8), A_c is the microchannel's cross-sectional area and P_w is its wetted perimeter.

The Reynolds number describes the fluid flow; at low Reynolds, the flow is laminar, whereas high Reynolds indicates turbulent flow.

2.1. Geometry and design principle

A schematic of the micromixer's design including the microchannel dimensions in millimeter is depicted in Fig. 1.

The design is chosen to be curved such that a rather strong secondary flow would develop within the microchannel. In curved microchannels, the fluid undergoes a secondary flow created due to the Dean-flow effect. This secondary flow is comprised of two tangentially opposite vortices and is perpendicular to the original flow in the microchannel's axial direction. The vortices cause the fluids to be mixed through stirring them together within a swirling motion.

This swirling motion which the fluid experiences as it passes through a curved path is often known as the Dean flow. The dimensionless Dean number is defined as Eq. (9):

$$De = Re \sqrt{\frac{D_h}{2R_c}} \quad (9)$$

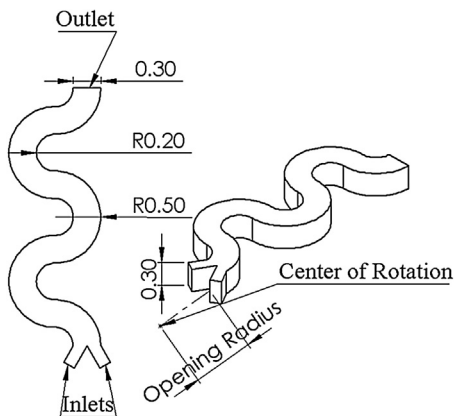


Fig. 1. Schematic of the micromixer's design with dimensions in mm.

where R_c is the microchannel's radius of curvature (m). In rectilinear microchannels such as La et al.'s [37], the radius of curvature is infinity (except at sharp corners where R_c has a singularity), thus Dean number is zero. In these channels, the stirring effect happens solely due to the Coriolis force occurring within an LOCD platform due to its rotation. However, in curved microchannels such as ours, the radius of curvature could be designed to be in the order of the microchannel's hydraulic diameter; therefore, the Dean number could take significant values. The higher the Dean number is, the stronger are the Dean and the secondary flow, hence, mixing is enhanced. In contrast to straight or rectilinear microchannels which could only benefit from the Coriolis force to induce the secondary flow, curved microchannels innately actualize the Dean flow as the fluid flows through the curved path, coming to the aid of Coriolis force and significantly enhancing the stirring of the fluids and mixing.

2.2. Boundary conditions

The no-slip boundary condition was exerted on the microchannel walls for the fluid flow study. At the inlets and the outlet, constant zero gauge pressure was maintained. The working fluid was selected to be deionized water with a density of 1000 kg/m^3 and a dynamic viscosity of 0.001 Pa s . The no-mass flux boundary condition was applied to the walls for the mass transfer study. Constant concentrations of 0 and 1 were designated at the inlets. A diffusivity constant of $1.67 \times 10^{-9} \text{ m}^2/\text{s}$ was selected to be consistent with La et al.'s experiment [37], such that it would allow further result comparisons.

2.3. Numerical method

The Finite Element Method was employed to numerically solve the governing equations using COMSOL Multiphysics software. A uniform, structured mesh was built to discretize the computational domain of the problem. The grid had to be uniform because Eq. (7), which was employed to calculate the Mixing Quality, is defined within the discrete space of computational cells. Hence, the computational cells need have equal sizes. Structured hexahedral meshes were applied to all the studied mixer geometries. The gridlines in the computational domain were considered to be aligned with or orthogonal to the flow direction in order to ensure the accuracy of the numerical solution [45]. In a Cartesian grid, false diffusion, which is an inevitable byproduct of the numerical simulations, maximizes when the angle between the gridlines and the flow direction is 45° , whereas, the minimum false diffusion occurs when the gridlines are aligned with or orthogonal to the flow direction [46].

3. Results and discussion

With all aforementioned considerations, simulations were run for different setups of the problem. Analyses were conducted for grid sensitivity, validation, effect of curvature, effect of angular velocity and effect of opening radius. The results are brought in their own respective sections below in the format of Mixing Quality varied as a dependent variable against each section's independent variable.

3.1. Grid sensitivity analysis

In this section, the solution's sensitivity to the number of grids in the computational domain is investigated. In order to assess the grid sensitivity, three case studies with total cell numbers of 330,510, 783,200 and 1,324,600 were carried out. The results for

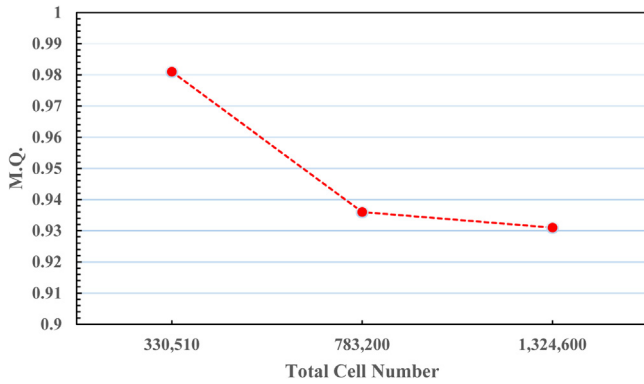


Fig. 2. M.Q. vs. total cell number for analyzing grid sensitivity.

this inquiry are depicted in Fig. 2 where the Mixing Quality is plotted against total cell number. As is observed in Fig. 2, after increasing the number of computational cells to 783,200 cells, the mixing quality no longer changes; thus, mesh independency is ensured.

3.2. Validation analysis

The simulation results were validated against La et al.'s experimental data [37]. For this purpose, an identical simulation of La's study was run. The model geometry was extracted from La's

experimental setup. The mesh selected for this study is illustrated in Fig. 3 along with a magnified region.

To conduct the validation analysis, the same conditions present in all other simulations were maintained (e.g. problem physics, boundary conditions) and a simulation was run. As a graphic result, the concentration contour for this simulation is presented in Fig. 4a.

Fig. 4b depicts a plot of Mixing Quality versus down-channel length for our simulation against La's experiment, enabling a quantitative comparison. As is displayed in Fig. 4b, a satisfactory agreement is yielded between our validation simulation with La's experimental results. This guarantees the physical validity of this study. The calculated mixing quality shows a slightly oscillatory behavior in terms of the rate of increase for the mixing quality. Vertical dash-dot lines in Fig. 4b correspond to the locations of certain bends in the microchannel which are designated with arrows in Fig. 4a and enumerated in Fig. 4b. As is observed in Fig. 4b, noticeable ascents have occurred at bends 1 and 3 while no such ascent has occurred at bends 2 and 4. To put it in terms of Mixing Quality, bends 1 and 3 have caused substantial increases in the rate of Mixing Quality while no similar increase in rate is noticed in bends 2 and 4. The reason behind this phenomenon is that within bends 1 and 3, the Coriolis Force is parallel with the secondary flow and in its same direction, thus intensifying the secondary flow and subsequently the mixing rate. However, in bends 2 and 4 the Coriolis Force is in the opposite direction with the secondary flow, thus weakening the secondary flow and subsequently lowering the mixing rate. Yet due to the existence of

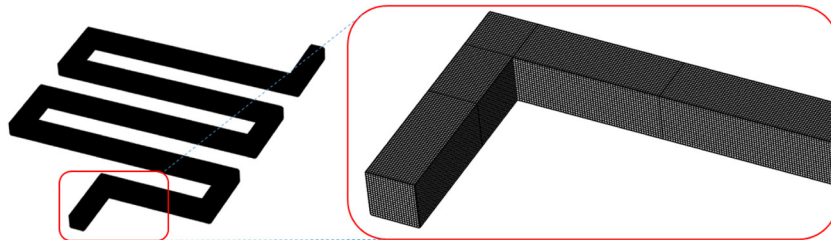


Fig. 3. Selected mesh for validation analysis with a magnified region.

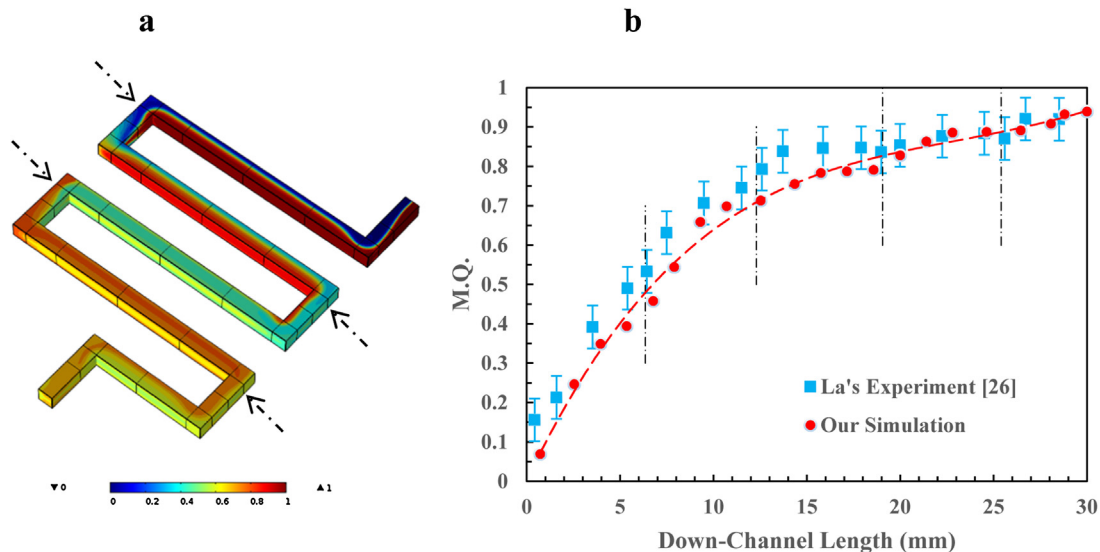


Fig. 4. a. Concentration contour for validation simulation. b. M.Q. vs. down-channel length for validation analysis, the long-dashes line is the curve fitted to the calculated M.Q.

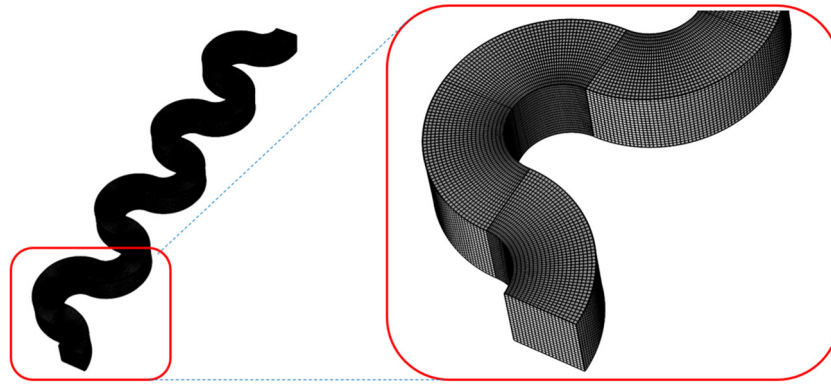


Fig. 5. The employed structured mesh with a magnified region.

the secondary flow all throughout the microchannel, the mixing rate stays positive and Mixing Quality increases with down-channel length. The employed structured grid for the following studies is depicted in Fig. 5.

3.3. Effect of curvature

In this section, microchannel curvature is introduced as a design parameter affecting mixing. Thereafter, the effect of curvature of a curved, serpentine microchannel on mixing performance was studied.

Furthermore, the numerical results obtained for both the rectilinear microchannel and the serpentine design are compared to each other. The calculated Mixing Quality for La's rectilinear microchannel and our serpentine design with the same down-channel length are plotted in Fig. 6.

As is observed, the curvature significantly enhances mixing. With a more careful examination of Fig. 6, it can be found that the successive changes of the fluid's direction in the serpentine design lead to the high performance of the device. Specifically, those bends in which the Coriolis force is in the same direction with the secondary flow, function as great mixing enhancers. This is noticed in Fig. 6 in which rather steep ascents in the mixing quality correspond to locations of these bends. Yet the steep ascents vanish as the mixing quality increases asymptotically, i.e. the increase rate diminishes gradually, within the concluding sections of the

microchannel. It is noticed that after the fluid has passed through 10 mm of the microchannel's length, while our curved micromixer's M.Q. reaches almost 90%, La's rectilinear micromixer barely reaches 70%. Moreover, the curved design is discerned to be superior at every single section down the microchannel's length, mixing-wise. One better fathoms this superiority once one appreciates the fact that La's micromixer reaches 90% M.Q. only after the fluid has passed through 30 mm of down-channel length according to Shamloo et al. [43]. This means our curved micromixer reaches felicitous mixing performance within barely one third of La's required down-channel length for sufficient mixing. The reason for this phenomenon is that when the microchannel is curved, an enhanced Dean flow arises which subsequently constitutes a strong secondary flow. As was mentioned earlier, the secondary flow shapes up as two adjacent, opposite vortices perpendicular to the axial flow, intensifying mixing through fluid stirring. Fig. 7 illustrates the concentration contour for the curved micromixer along with cross-sections depicting the aforementioned vortices.

3.4. Effect of angular velocity

Here we have studied the effect of the angular velocity parameter on mixing performance. As it was discussed in the study conducted by Shamloo et al. [43], increasing the angular velocity continuously improves mixing. However, in this work a broader range of angular velocities was selected and a quite different mixing behavior was noticed. Fig. 8 displays Mixing Quality vs angular velocity over a broad range from 7.5 rad/s to 350 rad/s. Moreover, Table 1 lines up values for volume flow rate, average velocity and dimensionless numbers Reynolds and Dean against angular velocity over the studied range. All data were calculated at the microchannel's outlet.

As is observed in Fig. 8, the Mixing Quality drops with increasing angular velocity at low regions and upon reaching a minimum, begins to continuously increase with increasing angular velocity. The reason for this phenomenon is that at low angular velocities, the Reynolds number and subsequently the Dean number are rather small. Within these regions, the dominant mixing mechanism is simply diffusion. Through diffusion, the two to-be-mixed fluids disperse and diffuse within one another naturally. However, this process is extremely time consuming; such that a solely diffusion-based micromixer would not be efficient for industrial or laboratory purposes. Upon increasing angular velocity beyond a certain value though, which we have called "threshold angular velocity", the secondary flow created due to the curvature and the imposed Coriolis force takes over and becomes the dominant mixing mechanism. Therefore, in regions with angular velocities above this threshold, the M.Q. continuously

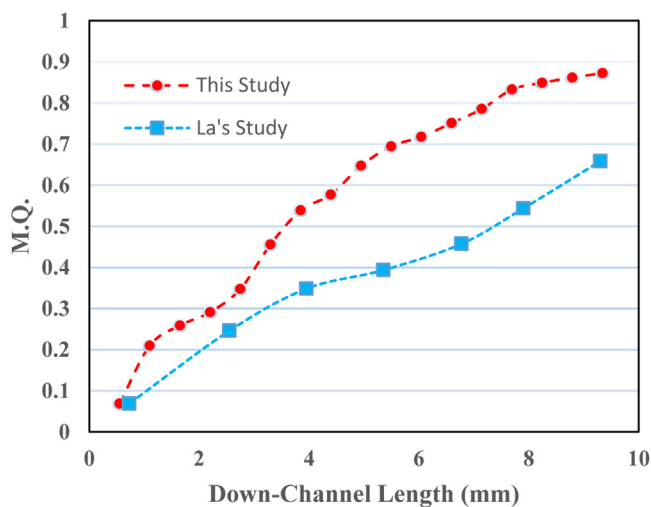


Fig. 6. M.Q. obtained by the numerical simulation along the down-channel length for our curved design and La's rectilinear design; dash line is the curve fitted to the numerical results.

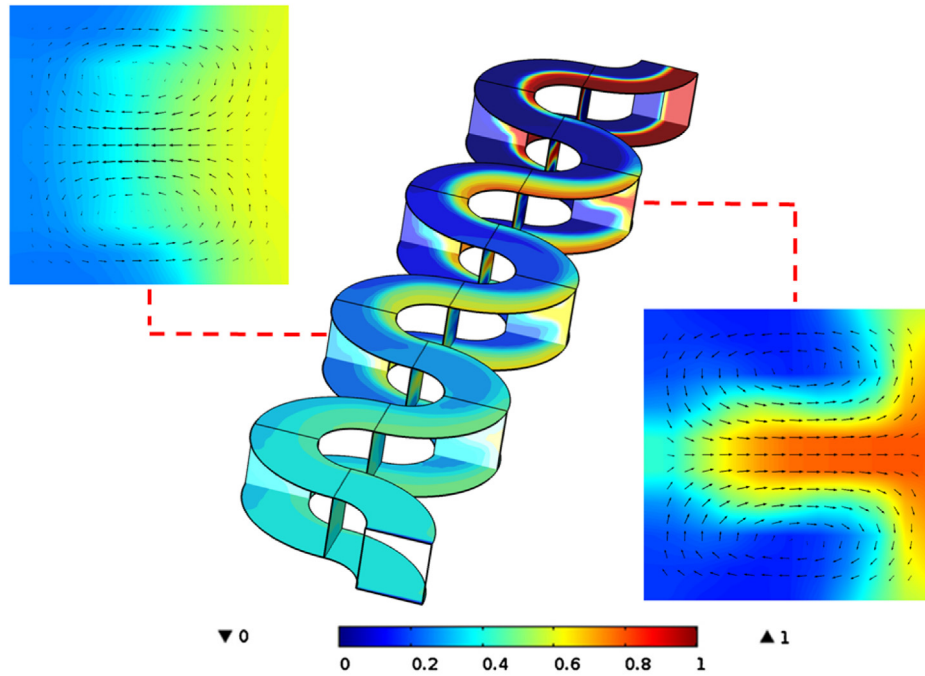


Fig. 7. Concentration contour along with cross-sections depicting secondary flow.

increases with angular velocity. The value of the threshold angular velocity in our study was found to be 50 rad/s which corresponds to a Dean number of 1.4. Above this Dean number, increasing angular velocity continuously enhances mixing. In simple LOCs which do not employ centrifugal rotation, secondary flow becomes dominant only at Dean Numbers around 10 (Kim and Lee [47], Yoon et al. [48]). However, since our design utilizes centrifugal rotation, the Coriolis force comes to the aid of Dean Flow and they both enhance the secondary flow together, causing it to take over at much lower Dean numbers, here being 1.4. Furthermore, the obtained threshold angular velocity of 50 rad/s is lower than the angular velocity with which the study of this parameter had simply begun in the study of Shamloo et al. [43]. This means that the trend with which mixing performance drops against increasing angular velocity in regions below the threshold could have simply never been realized in that study. Also the existence of a threshold angular velocity at which the secondary flow becomes dominant against diffusion was also never addressed in the past studies.

As one may notice in Table 1, the M.Q. has reached values close to unity for extremely low angular velocities, which seems too good to be true, and it is. Of course reaching such M.Q. is indefinitely desirable for a micromixer, yet it is essential for the

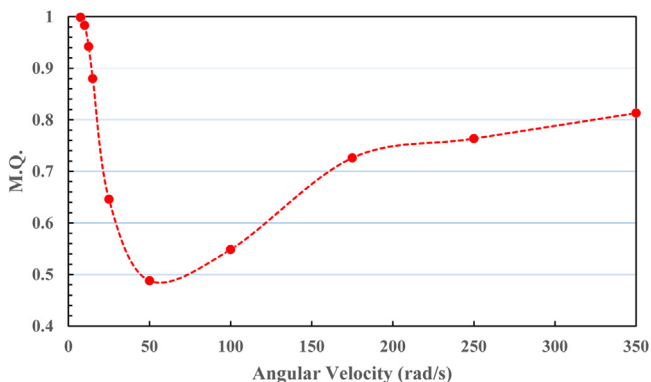


Fig. 8. M.Q. vs. angular velocity.

same micromixer to be able to produce that M.Q. in appropriate time. The pure diffusion process is extremely slow compared with the fluid stirring occurring in secondary-flow micromixers where mixing occurs much more rapidly. Since the governing equations in this study were carried out in steady-state and time-independent, the M.Q. alone cannot distinguish between the mixing behaviors in high and low angular velocities, which differ greatly over residence time of the fluid in the mixer. To explicitly address this difference, values of average fluid velocity are charted in Table 1. Each value corresponds to a specific angular velocity. Because of continuity in an incompressible flow and the fact that the cross-sectional area does not vary throughout the microchannel's length, the average fluid velocity remains unchanged within its path in the microchannel. Therefore, the average velocity with which the fluid has passed through the microchannel is the same as the average velocity it has at the end of the microchannel, which is listed in Table 1.

Another important parameter that should be taken into consideration is the average residence time for the fluid passing through the mixer. The residence time for an entirely diffusive system is simply defined as real time, however, for a convective-diffusive system, it is called space-time [49]. The space-time is defined as

$$\tau = \frac{V}{Q} \quad (10)$$

where V denotes the volume (m^3) of the mixer, and Q is the volumetric flow rate ($\frac{\text{m}^3}{\text{s}}$) of the working fluids. In order to compare the residence time for the mixer with different angular velocities, two extremes were considered. The purely diffusive and the convective-diffusive mixing processes with angular velocities of 7.5 rad/s and 350 rad/s, respectively. Now, Eq. (11) calculates the residence time of the fluid for these two extremes.

$$\frac{\tau_{\omega=7.5}}{\tau_{\omega=350}} = \frac{Q_{\omega=350}}{Q_{\omega=7.5}} \approx 1420 \quad (11)$$

This means, the residence time of the fluids in the mixer with the angular velocity of 7.5 rad/s is approximately 1420 times of that for

Table 1
Assessment of flow parameters against angular velocity.

ω (rad/s)	M.Q. (%)	Q (m ³ /s)	U _{avg} (m/s)	Re	De
7.5	99.8	1.48×10^{-11}	1.6×10^{-4}	0.05	0.03
10	98.3	2.62×10^{-11}	2.9×10^{-4}	0.09	0.06
12.5	94.2	4.10×10^{-11}	4.6×10^{-4}	0.14	0.09
15	87.9	5.90×10^{-11}	6.6×10^{-4}	0.20	0.13
25	64.5	1.64×10^{-10}	1.8×10^{-3}	0.55	0.36
50	48.7	6.57×10^{-10}	7.3×10^{-3}	2.19	1.43
100	54.8	2.62×10^{-9}	2.9×10^{-3}	8.74	5.72
175	72.6	1.21×10^{-8}	1.3×10^{-2}	40.41	26.45
250	76.3	1.29×10^{-8}	1.4×10^{-2}	42.94	28.11
350	81.3	2.10×10^{-8}	2.3×10^{-2}	70.01	45.83

the mixer with the angular velocity of 350 rad/s. This is why pure-diffusion micromixers are neither practical nor efficient.

It is also noted in Table 1 that the values for Dean Number in this study are significantly greater than typical microfluidics. The Dean Number, as mentioned earlier, is defined as Eq. (9):

$$De = Re \sqrt{\frac{D_h}{2R_c}} = Re \sqrt{\frac{300}{2 \times 350}} \cong 0.65Re \quad (9)$$

in this study, the hydraulic diameter D_h and the microchannel's radius of curvature R_c were selected to be in the same order ($D_h = 300 \mu\text{m}$ and $R_c = 350 \mu\text{m}$). This way their ratio remains a constant close to unity, therefore, Dean grows with increasing Reynolds of the flow. This design criterion is key to achieving higher Dean Numbers and subsequently, stronger secondary flows.

3.5. Effect of opening radius

In this section we have investigated the effect of the opening radius, i.e. the original radius at which the micromixer unit starts on the LOCD. In a centrifugal LOCD setup, the further the fluid is from the center of the disk, the higher would be its velocity; therefore, this original radius is assumed to affect mixing. Fig. 9 displays a plot of Mixing Quality vs. opening radius plotted for a range of original radii from 1 cm to 4 cm. It is noticed that M.Q. increases with increasing original radius. In higher original radii, the fluid velocity is larger, so is the Reynolds and subsequently Dean number. For a larger original radius, a stronger secondary flow develops within the fluid, thus enhancing the mixing. However, it is noticed that increasing the opening radius simply slightly improves mixing. As is displayed in Fig. 9, increasing the opening radius fourfold barely increases mixing quality by 10% which is simply not enough at the expense of a compact design. Since an LOCD may have to host operational units other than

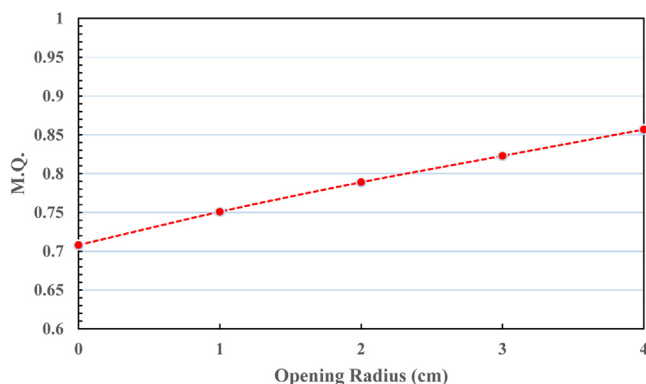


Fig. 9. M.Q. vs. Opening Radius.

mixing, such as valving or separation (Kirby et al. [50]), to which the mixing unit is prior, a compact micromixer design is always preferred in LOCDs. Hence, increasing the opening radius in order to get better mixing is not practical.

4. Conclusion

In this paper a centrifugal, serpentine micromixer was investigated along with modifications which enhanced mixing performance. The micromixer was given a curved design since it was realized that because of a strong Dean flow induced due to the curvature, the curved micromixer functions quite superiorly to a typical, rectilinear design. To put it quantitatively, the curved design reaches 90% M.Q. within 10 mm of down-channel length, whereas the equivalent rectilinear design reaches it in 30 mm. This means the curved design is three times as functional and compact, from a geometric design perspective. The effect of angular velocity of the LOCD on mixing performance was comprehensively studied. It was gathered that mixing performance drops with increasing angular velocity until it reaches a minimum at a threshold angular velocity. The threshold angular velocity was found to be 50 rad/s at which the dominant mixing regime changes from diffusion to secondary flow. Above this threshold, the secondary flow overcomes the diffusion and mixing performance begins to continuously increase with angular velocity. In post-threshold regions, a higher angular velocity develops a stronger secondary flow which leads to significantly improved mixing. Finally, the effect of opening radius, i.e. the radius at which the micromixer unit begins on the LOCD, was studied in a similar fashion. It was realized that while increasing the opening radius enhances mixing performance, this enhancement is rather insignificant and since it occurs at the expense of a compact design, it is not regarded as a practical means to enhance mixing. All in all, it is concluded that a curved, centrifugal micromixer with an appropriate angular velocity could yield felicitous mixing performance within a compact-design LOCD setup. Computational fluid dynamics is a powerful tool for studying fluid flow behavior in microfluidic devices. In future studies, we aim to enhance the performance of different microfluidics by experimentally implementing the microfluidic devices investigated in this study and our previous studies [51–54].

References

- [1] D. Figeys, D. Pinto, Lab-on-a-chip: a revolution in biological and medical sciences, *Anal. Chem.* 72 (2000) 330A–335A.
- [2] S. Haeberle, T. Brenner, H.P. Schlosser, R. Zengerle, J. Duerée, Centrifugal micromixery, *Chem. Eng. Technol.* 28 (2005) 613–616.
- [3] S.-J. Lee, B.-K. Choi, The artificial glomerulus design using diffusion in microchannels, *Int. J. Precis. Eng. Manuf.* 13 (2012) 307–310.
- [4] C.D. Chin, V. Linder, S.K. Sia, Lab-on-a-chip devices for global health: past studies and future opportunities, *Lab Chip* 7 (2007) 41–57.
- [5] S.-P. Ryu, J.-Y. Park, S.-Y. Han, Optimum design of an active micro-mixer using successive Kriging method, *Int. J. Precis. Eng. Manuf.* 12 (2011) 849–855.
- [6] V. Srinivasan, V.K. Pamula, R.B. Fair, An integrated digital microfluidic lab-on-a-chip for clinical diagnostics on human physiological fluids, *Lab Chip* 4 (2004) 310–315.
- [7] R.B. Fair, Digital microfluidics: is a true lab-on-a-chip possible? *Microfluid. Nanofluid.* 3 (2007) 245–281.
- [8] O. Strohmeier, M. Keller, F. Schwemmer, S. Zehnle, D. Mark, F. von Stetten, et al., Centrifugal microfluidic platforms: advanced unit operations and applications, *Chem. Soc. Rev.* 44 (2015) 6187–6229.
- [9] J. Duerée, S. Haeberle, S. Lutz, S. Pausch, F. Von Stetten, R. Zengerle, The centrifugal microfluidic Bio-Disk platform, *J. Micromech. Microeng.* 17 (2007) S103.
- [10] M. Grumann, A. Geipel, L. Riegger, R. Zengerle, J. Duerée, Batch-mode mixing on centrifugal microfluidic platforms, *Lab Chip* 5 (2005) 560–564.
- [11] M. Amasia, M. Madou, Large-volume centrifugal microfluidic device for blood plasma separation, *Bioanalysis* 2 (2010) 1701–1710.
- [12] J. Siegrist, R. Gorkin, L. Clime, E. Roy, R. Peytavi, H. Kido, et al., Serial siphon valving for centrifugal microfluidic platforms, *Microfluid. Nanofluid.* 9 (2010) 55–63.
- [13] S. Haeberle, R. Zengerle, J. Duerée, Centrifugal generation and manipulation of droplet emulsions, *Microfluid. Nanofluid.* 3 (2007) 65–75.

- [14] P. Roy, N. Anand, D. Banerjee, A review of flow and heat transfer in rotating microchannels, *Procedia Eng.* 56 (2013) 7–17.
- [15] B.S. Lee, Y.U. Lee, H.-S. Kim, T.-H. Kim, J. Park, J.-G. Lee, et al., Fully integrated lab-on-a-disc for simultaneous analysis of biochemistry and immunoassay from whole blood, *Lab Chip* 11 (2011) 70–78.
- [16] D.S. Kim, S.W. Lee, T.H. Kwon, S.S. Lee, A barrier embedded chaotic micromixer, *J. Micromech. Microeng.* 14 (2004) 798.
- [17] S. Lai, S. Wang, J. Luo, L.J. Lee, S.-T. Yang, M.J. Madou, Design of a compact disk-like microfluidic platform for enzyme-linked immunosorbent assay, *Anal. Chem.* 76 (2004) 1832–1837.
- [18] G. Jia, K.-S. Ma, J. Kim, J.V. Zoval, R. Peytavi, M.G. Bergeron, et al., Dynamic automated DNA hybridization on a CD (compact disc) fluidic platform, *Sens. Actuators B: Chem.* 114 (2006) 173–181.
- [19] R. Gorkin, J. Park, J. Siegrist, M. Amasia, B.S. Lee, J.-M. Park, et al., Centrifugal microfluidics for biomedical applications, *Lab Chip* 10 (2010) 1758–1773.
- [20] M.J. Madou, L.J. Lee, S. Daunert, S. Lai, C.-H. Shih, Design and fabrication of CD-like microfluidic platforms for diagnostics: microfluidic functions, *Biomed. Microdevices* 3 (2001) 245–254.
- [21] Z. Noroozi, H. Kido, M. Micic, H. Pan, C. Bartolome, M. Princevac, et al., Reciprocating flow-based centrifugal microfluidics mixer, *Rev. Sci. Instrum.* 80 (2009) 075102.
- [22] S. Chakraborty, *Microfluidics and Microscale Transport Processes*, CRC Press, 2012.
- [23] Y. Wang, J. Zhe, B.T. Chung, P. Dutta, A rapid magnetic particle driven micromixer, *Microfluid. Nanofluid.* 4 (2008) 375–389.
- [24] H.-Y. Wu, C.-H. Liu, A novel electrokinetic micromixer, *Sens. Actuators A: Phys.* 118 (2005) 107–115.
- [25] T. Tofteberg, M. Skolimowski, E. Andreassen, O. Geschke, A novel passive micromixer: lamination in a planar channel system, *Microfluid. Nanofluid.* 8 (2010) 209–215.
- [26] V. Hessel, H. Löwe, F. Schönfeld, Micromixers—a review on passive and active mixing principles, *Chem. Eng. Sci.* 60 (2005) 2479–2501.
- [27] A.D. Stroock, S.K. Dertinger, A. Ajdari, I. Mezić, H.A. Stone, G.M. Whitesides, Chaotic mixer for microchannels, *Science* 295 (2002) 647–651.
- [28] Y.-S. Chen, H.-S. Liu, C.-C. Lin, W.-T. Liu, Micromixing in a rotating packed bed, *J. Chem. Eng. Jpn.* 37 (2004) 1122–1128.
- [29] J. Ducree, T. Brenner, S. Haerberle, T. Glatzel, R. Zengerle, Multilamination of flows in planar networks of rotating microchannels, *Microfluid. Nanofluid.* 2 (2006) 78–84.
- [30] C.H. Shih, C.H. Lu, C.H. Lin, H.J. Wu, Design and analysis of micromixers on a centrifugal platform, *Adv. Mater. Res.* (2009) 203–206.
- [31] M.C. Kong, E.D. Salin, Micromixing by pneumatic agitation on continually rotating centrifugal microfluidic platforms, *Microfluid. Nanofluid.* 13 (2012) 519–525.
- [32] Y. Ren, W.W.-F. Leung, Numerical and experimental investigation on flow and mixing in batch-mode centrifugal microfluidics, *Int. J. Heat Mass Transfer* 60 (2013) 95–104.
- [33] C.-H. Shih, H.-C. Chang, W.-L. Yuan, C.-H. Lin, H.-C. Wu, Design and fabrication of a rapid micromixer on a centrifugal platform, *J. Nanosci. Nanotechnol.* 16 (2016) 7037–7042.
- [34] D.C. Duffy, H.L. Gillis, J. Lin, N.F. Sheppard, G.J. Kellogg, Microfabricated centrifugal microfluidic systems: characterization and multiple enzymatic assays, *Anal. Chem.* 71 (1999) 4669–4678.
- [35] L.G. Puckett, E. Dikici, S. Lai, M. Madou, L.G. Bachas, S. Daunert, Investigation into the applicability of the centrifugal microfluidics platform for the development of protein-ligand binding assays incorporating enhanced green fluorescent protein as a fluorescent reporter, *Anal. Chem.* 76 (2004) 7263–7268.
- [36] J.V. Zoval, M.J. Madou, Centrifuge-based fluidic platforms, *Proc. IEEE* 92 (2004) 140–153.
- [37] M. La, S.J. Park, H.W. Kim, J.J. Park, K.T. Ahn, S.M. Ryew, et al., A centrifugal force-based serpentine micromixer (CSM) on a plastic lab-on-a-disk for biochemical assays, *Microfluid. Nanofluid.* 15 (2013) 87–98.
- [38] L. Falk, J.-M. Commenge, Performance comparison of micromixers, *Chem. Eng. Sci.* 65 (2010) 405–411.
- [39] W. Ehrfeld, K. Golbig, V. Hessel, H. Löwe, T. Richter, Characterization of mixing in micromixers by a test reaction: single mixing units and mixer arrays, *Ind. Eng. Chem. Res.* 38 (1999) 1075–1082.
- [40] J. Aubin, D.F. Fletcher, J. Bertrand, C. Xuereb, Characterization of the mixing quality in micromixers, *Chem. Eng. Technol.* 26 (2003) 1262–1270.
- [41] J. Zalc, E. Szalai, F. Muzzio, S. Jaffer, Characterization of flow and mixing in an SMX static mixer, *AIChE J.* 48 (2002) 427–436.
- [42] P. Danckwerts, The definition and measurement of some characteristics of mixtures, *Appl. Sci. Res. Sec. A* 3 (1952) 279–296.
- [43] A. Shamloo, M. Madadelahi, A. Akbari, Numerical simulation of centrifugal serpentine micromixers and analyzing mixing quality parameters, *Chem. Eng. Process. Process Intensif.* 104 (2016) 243–252.
- [44] K. Malecha, L.J. Golonka, J. Baidyga, M. Jasińska, P. Sobieszuk, Serpentine microfluidic mixer made in LTCC, *Sens. Actuators B* 143 (2009) 400–413.
- [45] S. Patankar, *Numerical Heat Transfer and Fluid Flow*, CRC press, 1980.
- [46] R.T. Bailey, Managing false diffusion during second-order upwind simulations of liquid micromixing, *Int. J. Numer. Methods Fluids* (2016).
- [47] S. Kim, S.J. Lee, Measurement of Dean flow in a curved micro-tube using micro digital holographic particle tracking velocimetry, *Exp. Fluids* 46 (2009) 255–264.
- [48] D.H. Yoon, J.B. Ha, Y.K. Bahk, T. Arakawa, S. Shoji, J.S. Go, Size-selective separation of micro beads by utilizing secondary flow in a curved rectangular microchannel, *Lab Chip* 9 (2009) 87–90.
- [49] D. Gobby, P. Angeli, A. Gavriilidis, Mixing characteristics of T-type microfluidic mixers, *J. Micromech. Microeng.* 11 (2001) 126.
- [50] D. Kirby, J. Siegrist, G. Kijanka, L. Zavattoni, O. Sheils, J. O'Leary, et al., Centrifugo-magnetophoretic particle separation, *Microfluid. Nanofluid.* 13 (2012) 899–908.
- [51] A. Shamloo, M. Mirzakanloo, M.R. Dabirzadeh, Numerical simulation for efficient mixing of Newtonian and non-Newtonian fluids in an electro-osmotic micro-mixer, *Chem. Eng. Process. Process Intensif.* 107 (2016) 11–20.
- [52] A. Shamloo, P. Vatankhah, M.A. Bijarchi, Numerical optimization and inverse study of a microfluidic device for blood plasma separation, *Eur. J. Mech.* 57 (2016) 31–39.
- [53] A. Shamloo, A.A. Selahi, M. Madadelahi, Designing and modeling a centrifugal microfluidic device to separate target blood cells, *J. Micromech. Microeng.* 26 (2016) 035017.
- [54] A. Shamloo, F. Sharifi, S.S. Salehi, L. Amirifar, B. Firoozabadi, Performance optimization of microreactors by implementing geometrical and fluid flow control in the presence of electric field: a computational study, *Microsys. Tech.* 21 (2015) 1275–1285.



Amir Shamloo received his Ph.D. from Stanford University, Stanford, CA, 2010. He was a postdoctoral scholar at the University of California, Berkeley, CA. He is now an associate professor at the mechanical engineering department of Sharif University of Technology. His research involves the design and fabrication of microfluidic devices and their application in biology.



Parham Vatankhah received his B.Sc. degree in Mechanical Engineering from University of Tehran in 2013 and now he is M.Sc. candidate at the Mechanical Engineering department of Sharif University of Technology. His research interests include CFD simulations, design and fabrication of microfluidic devices and heat transfer in nanofluids.



Ali Akbari received his B.Sc. degree in Mechanical Engineering from Sharif University of Technology in 2014 and now he is an M.Sc. candidate at the Mechanical Engineering department of Sharif University of Technology. His research interests include CFD simulations and Bio-fluids.